J Mater Sci (2007) 42:9559–9564
DOI 10.1007/s10853-007-1895-0

INTERFACE SCIENCE

Local structure modulation of the low La-doped layered strontium manganite $Sr_4Mn_3O_{10}$ studied by transmission electron microscopy and electron energy-loss spectroscopy

H. Yang · Y. K. Tang · J. L. Jiang · W. J. Feng · Z. Q. Wei · L. D. Yao · W. Zhang · Q. A. Li · F. Y. Li · C. Q. Jin · R. C. Yu

Received: 12 March 2007 / Accepted: 29 May 2007 / Published online: 27 July 2007

Abstract Transmission electron microscopy (TEM) and electron energy-loss spectroscopy (EELS) have been used to characterize the structure and microstructure of the low La-doped layered manganite $La_xSr_{4-x}Mn_3O_{10}$ ($x \leq 0.15$). The structure of the perfect phase has been identified as an $n = 3$ layered structure of the hexagonal series by electron diffraction (ED), high-resolution electron microscopy (HRTEM) together with numerical image simulations. The presence of local superstructure modulation associated with La ordering in the compounds was revealed by electron diffraction and high-resolution electron microscopy. Electron diffraction data indicate that this superstructure modulation is two-dimensional, and the modulation plane lies in the *ac* plane. The two primary modulation vectors are $q_1 = (1/4)a^*$ and $q_2 = (1/2)c^*$. In addition, another type of modulated structure associated with *periodic* lattice distortion was occasionally visible in the $La_{0.15}Sr_{3.85}Mn_3O_{10}$ phase. Energy-loss spectroscopy data indicate that the *periodic* lattice distortion is led by ordered oxygen deficiency.

H. Yang · J. L. Jiang · W. J. Feng · Z. Q. Wei
School of Science, Lanzhou University of Technology, Gansu Lanzhou 730050, P.R. China

H. Yang · L. D. Yao · W. Zhang · F. Y. Li · C. Q. Jin · R. C. Yu (✉)
Laboratory for Extreme Condition Physics, Beijing National Laboratory for Condensed Matter Physics, Institute of Physics, Chinese Academy of Sciences, P. O. Box 603, Beijing 100080, P.R. China
e-mail: rcyu@aphy.iphy.ac.cn

Y. K. Tang · Q. A. Li
State Key Laboratory of Magnetism, Beijing National Laboratory for Condensed Matter Physics, Institute of Physics, Chinese Academy of Sciences, P. O. Box 603, Beijing 100080, P.R. China

Introduction

Perovskite-based manganites have received considerable interest in recent years since the discovery of colossal magnetoresistance (CMR) effect in substituted $(R,A)MnO_3$ (R and A being trivalent rare-earth and divalent alkaline-earth ions, respectively) [1–3]. A number of works have been devoted to layered perovskite-based manganites with the general formula $(R,A)_{n+1}Mn_nO_{3n+1}$ aimed at understanding the influence of dimensionality on the magnetoresistance behavior. Structurally the $(R,A)_{n+1}Mn_nO_{3n+1}$ manganites have been shown to be able to crystallize in two kinds of layered structural type. One is representative of the Ruddlesden-Popper (RP) series [4] built up from n layers of perovskite blocks alternating with single $(R,A)O$ rock-salt layers. The other is generally called the hexagonal homologous series [5] which is based on such a building principle: blocks of n face-sharing $[MnO_6]$ octahedra linked one to each other by two of the three terminal corners forming a two-dimensional sheet (as an example, Fig. 1 shows the [100] projection of the $n = 3$ structure of this series).

For the $n = 3$ member of the RP series, some detailed works were reported about $Ca_4Mn_3O_{10}$ [6–8]. However, attempts to prepare $Sr_4Mn_3O_{10}$ and $Ba_4Mn_3O_{10}$ resulted in an $n = 3$ phase of the hexagonal series [9, 10]. The two manganites are isostructural to $Cs_4Ni_3F_{10}$ [11] and have the *Cmca* space group. Higher members of the hexagonal series, such as $Ba_6Mn_5O_{16}$ ($n = 5$) [12, 13], have also been

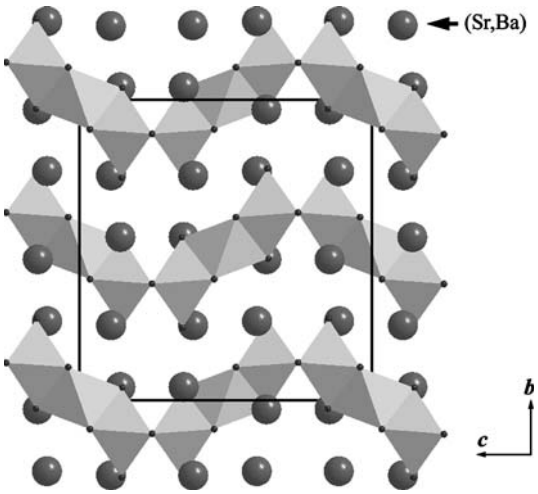

Fig. 1 [100] projection of the $n = 3$ structure of the hexagonal layered manganites, such as $Sr_4Mn_3O_{10}$ and $Ba_4Mn_3O_{10}$

stabilized. These hexagonal layered manganites were revealed by the magnetic measurements to be antiferromagnetic (AFM) insulators [9, 10, 12–14]. Up to now, despite many studies of the layered manganites belonging to the hexagonal series, little work has been concerned with the effects of rare earth doping on their structural and physical properties.

Recently, we have carried out investigations on structural and magnetic properties of the La-doped $La_xSr_{4-x}Mn_3O_{10}$. Single-phase samples were obtained for $x \leq 0.15$ based on the powder x-ray diffraction (XRD) data, and the magnetic measurements indicate that ferromagnetic (FM) clusters are induced in them by the slight doping of La [15]. Interestingly, albeit the low La-doped $La_xSr_{4-x}Mn_3O_{10}$ samples appear single phased from the XRD analysis [15], the presence of complex microstructure, such as the local ordering of La atoms and the ordered oxygen-deficient superlattice, etc., has been revealed by transmission electron microscopy (TEM). Similar local ordering was also studied by TEM in other perovskite-type manganites [16]. For perovskite-based manganites, beside the intrinsic parameters (e.g., the Mn^{4+}/Mn^{3+} ratio and the Mn–O–Mn bond angles, etc.), the microstructure of these materials has also been known to influence significantly their electrical transport and magnetic properties. For instance, oxygen deficiency was shown to result in the increase of sample resistivity and the shift of Curie temperature T_c to lower temperatures [17, 18]. Therefore, microstructural evaluations in perovskite manganites have become a subject of intense interest. In this paper, we report on the structural and microstructural properties of $La_xSr_{4-x}Mn_3O_{10}$ revealed by transmission electron microscopy and electron energy-loss spectroscopy (EELS).

Experimental

Polycrystalline samples of $La_xSr_{4-x}Mn_3O_{10}$ were synthesized by the standard oxide ceramic processing technique. A stoichiometric mixture of $SrCO_3$, $MnCO_3$, and La_2O_3 powders was well ground and calcined twice at 900 and 950 °C for 24 h. Then, the resulting powder was pressed into pellets and sintered at 1150, 1160, and 1250 °C for 24 h, respectively. Thin foils for electron diffraction (ED), high-resolution transmission electron microscopy (HRTEM) and EELS studies were prepared by crushing La-doped $Sr_4Mn_3O_{10}$ ceramic in an agate mortar filled with alcohol, and then dispersing the fine fragments suspended in alcohol on Cu grids coated with holey carbon support films. A Tecnai F20 field-emission transmission electron microscope, installed at Beijing Laboratory of Electron Microscopy, Beijing National Laboratory for Condensed Matter Physics, was used for the TEM studies. The value of the C_s (the spherical aberration coefficient of the objective lens) of the microscope is 1.2 mm. EELS experiments were carried out in image mode, and the acquisition period of the spectra is 4 s. All the TEM experiments were carried out at an acceleration voltage of 200 keV.

Results and discussion

The fundamental structure of the $La_xSr_{4-x}Mn_3O_{10}$ ($x \leq 0.15$) samples were first characterized by selected area electron diffraction and high-resolution TEM techniques. The resultant ED and HRTEM data indicated that the

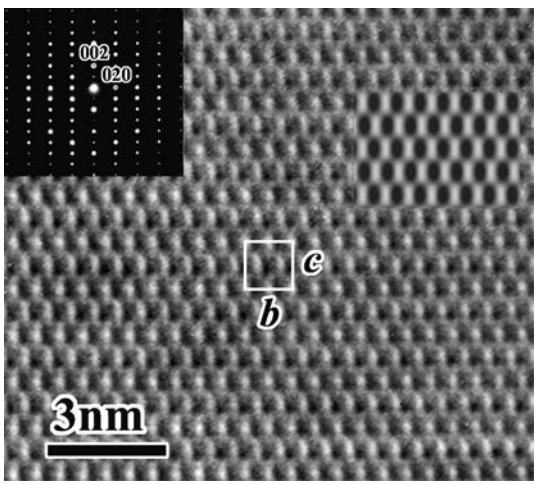

Fig. 2 [100] zone-axis HRTEM image obtained from the perfect phase of $La_xSr_{4-x}Mn_3O_{10}$ with $x = 0.15$. The corresponding ED pattern taken along the [100] direction is shown on the top left-hand corner of the image. No superstructure reflections ate visible in this zone axis. A simulated image is superimposed onto the experimental image

perfect $La_xSr_{4-x}Mn_3O_{10}$ phase has an $n = 3$ layered structure of the hexagonal series. Figure 2 shows a [100] zone-axis HRTEM image of the $x = 0.15$ sample. One unit cell is schematically outlined by a white solid line in the image. The corresponding ED pattern taken along the [100] zone-axis direction is shown on the top left-hand corner of Fig. 2, and also indicates the details about the layered structure. The camera length was calibrated using TlCl, and the lattice parameters were derived from ED patterns as: $a = 0.55$ nm, $b = 1.25$ nm and $c = 1.25$ nm, agreeing well with those refined from XRD data [15]. Assuming that Sr and La cations are statistically distributed over the same crystallographic sites, from the $Sr_4Mn_3O_{10}$ atomic coordinates [9], image simulations were carried out on the simulation program JEMS [19] using the multi-slice algorithm of dynamical scattering [20]. For image simulations the electron optical parameters of the microscope were used. The results showed that a simulated image for a defocus value of –70 nm and a thickness of 6 nm, superimposed onto the image, appears to be in agreement with the experimental one. In the $La_xSr_{4-x}Mn_3O_{10}$ phase, no intergrowth faults with different n members were observed, while such intergrowth faults were commonly visible in the $n = 5$ hexagonal phase $Ba_6Mn_5O_{16}$ [13]. We also attempted to synthesize $x > 0.15$ samples. However, no single-phase samples were obtained based on the XRD patterns that present extra diffraction peaks. Further investigations by TEM indicated that beside the major $n = 3$ hexagonal layered phase $(La,Sr)_4Mn_3O_{10}$, a minor $n = 2$ RP layered phase of $(La,Sr)_3Mn_2O_7$ and a minor rhombohedral ($R\bar{3}c$) phase of $(La,Sr)MnO_3$ were also formed in the $x > 0.15$ samples.

The presence of local superstructure modulation phenomenon in the $La_xSr_{4-x}Mn_3O_{10}$ manganite was found to be a striking feature resulting from the doping of La. The electron diffraction evidence for the superstructure modulation is given by the appearance of extra spots in addition to the fundamental reflections in the ED patterns. In the following, we proceed to discuss the results obtained for the typical sample with $x = 0.15$. Figure 3a presents a typical [010] zone-axis ED pattern taken on the modulated area. From the pattern, one can see that weak commensurate (or nearly commensurate) superstructure reflections appear not only along the a^* direction with a fourfold periodicity of d_{200}, but also along the c^* direction with a twofold periodicity of d_{002}. A microphotometric density line profile along the a^* direction is shown in Fig. 3b, displaying more clearly the superstructure reflections along this direction. Careful study of diffraction patterns along various orientations indicates that the structure modulation is two-dimensional, and the modulation plane lies in the a–c plane. Therefore, the superstructure reflections can be characterized by two primary modulation vectors $q_1 = (1/4)a^*$ and $q_2 = (1/2)c^*$, and their systematic positions can be described as $((1/2)n, 0, m,)$

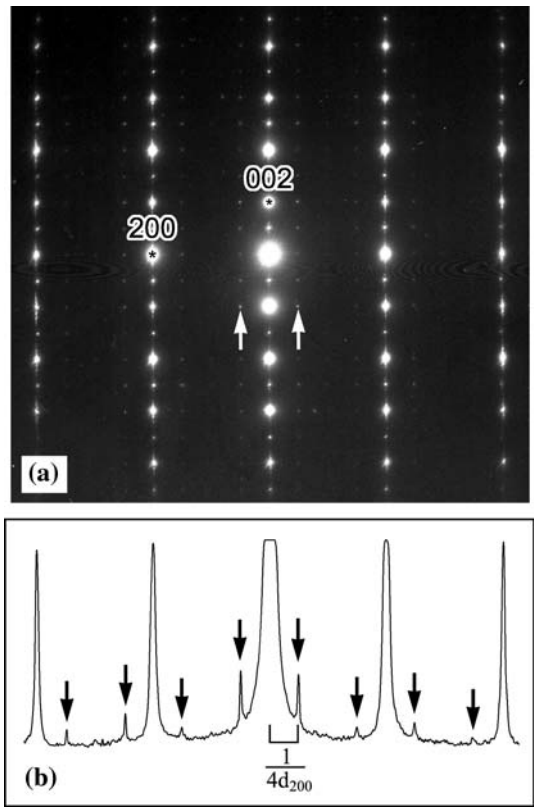

Fig. 3 (**a**) A typical [010] zone-axis ED pattern of $La_{0.15}Sr_{3.85}Mn_3O_{10}$, presenting weak superstructure reflections as indicated by the arrows. (**b**) A microphotometric density line profile along the a^* direction, displaying more clearly the superstructure reflections along this direction

where n and m are integers. In most cases, the ED patterns collected on the modulated areas present very weak superstructure reflections as shown by the example given in Fig. 3a, indicating a short-range coherent nature of the modulation. For a comparison we have also carried out TEM analyses on the undoped $Sr_4Mn_3O_{10}$ sample. However, no trace of any modulated structure was detected, which consists with the previous results obtained from $Sr_4Mn_3O_{10}$ [9]. This fact suggests that the appearance of the superstructure modulation in the $La_xSr_{4-x}Mn_3O_{10}$ manganite was caused obviously by the addition of La. Cation ordering (La/Sr) or charge ordering (Mn^{3+}/Mn^{4+}) are therefore considered to be the most possible factors resulting in the modulation.

High-resolution TEM experiments were also carried out to further investigate the superstructure modulation in the $La_xSr_{4-x}Mn_3O_{10}$ phase. Figure 4 shows a typical high-resolution TEM image taken along the [001] zone-axis direction, where the local superstructure modulation with a fourfold periodicity of d_{200} along the a^* direction is clearly visible. The modulation features, revealed from the image and also indicated by the corresponding fast Fourier transform (FFT) of the modulated structure (see the insert

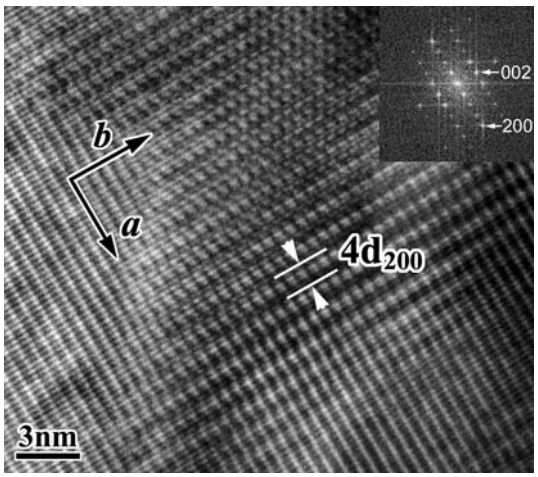

Fig. 4 A typical [001] HRTEM image of $La_{0.15}Sr_{3.85}Mn_3O_{10}$, where the local superstructure modulation with a fourfold periodicity of d_{200} along the a^* direction is clearly visible. This structure modulation is also indicated by the corresponding FFT

on the top right-hand corner of the image), consist with the results revealed by ED. This HRTEM image was obtained from a thick modulated region of the sample and does not provide enough information on the lattice configuration to help us explain the origin of the modulation. To clearly reveal the details of the modulation, it is required to obtain a high-quality HRTEM image from thin region of the crystal. Patient work performed in high-resolution TEM allowed us to obtain such an image as given in Fig. 5a. This image was taken along the [010] zone-axis direction. The corresponding FFT of the image is embedded on its top right-hand corner, indicating the typical characteristic of the two-dimensional superstructure modulation in the a–c plane. From this HRTEM image, one can see that the periodical distribution of the brightest spots, as indicated by the black arrows, is mainly attributed to the superstructure modulation. Further to discuss the origin of the modulation, it is necessary to properly correlate the spots with atomic-column positions in the image. It should be pointed out that this image was obtained under the defocus value of about –30 nm, which deviates from the Scherzer defocus (~ –60 nm) [21]. The crystal thickness as estimated from the low-loss EELS spectrum was ~5 nm. Under this circumstance, the projected rows of heavier atoms, such as La and Sr, appear as bright spots instead of dark ones. This was confirmed by image simulations based on the $Sr_4Mn_3O_{10}$ structure model [11], whose results suggested that in a simulated image for the defocus value of –30 nm and the thickness of 4.9 nm, as shown in Fig. 5b (the [010] projection of the $Sr_4Mn_3O_{10}$ structure is also superimposed on the simulated image), the Sr projected rows appear as bright spots. Based on this information, the brightest spots in the image are reasonably considered as the La-containing rows, and the brighter ones represent the Sr rows. This suggests that the orderly distribution of the La atoms is possibly a key factor resulting in the superstructure modulation. To unambiguously determine whether the La ordering is indeed the main mechanism for generating the modulated structure, a detailed image simulation is required. Such a simulation is challenging because it is difficult to properly model the La ordering. In the absence of suitable simulation, the ordering of the La atoms can be only said to be a most possible factor leading to the formation of the modulated structure.

Another type of modulated structure associated with *periodic* lattice distortion was occasionally visible in the $La_xSr_{4-x}Mn_3O_{10}$ phase. Figure 6 shows a [010] HRTEM image of this modulated structure. From the image as well as its corresponding FFT, one can see that structure modulation appears not only along the c^* direction with a nearly commensurate wave vector of $(1/2)c^*$, but also

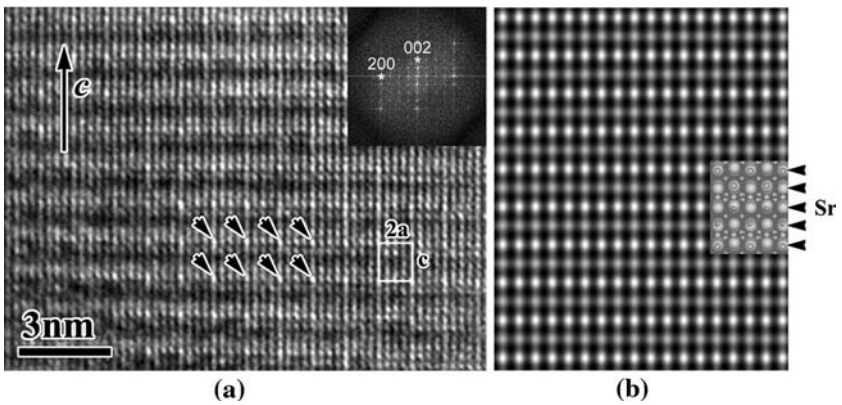

Fig. 5 (**a**) A [010] HRTEM image of $La_{0.15}Sr_{3.85}Mn_3O_{10}$, where one can see that the periodical distribution of the brightest spots, as indicated by the arrows, is mainly attributed to the superstructure modulation. The corresponding FFT of the image is embedded on its top right-hand corner, indicating the typical characteristic of the two-dimensional superstructure modulation in the a–c plane. (**b**) The simulated image for the defocus value of –30 nm and the thickness of 4.9 nm. The [010] projection of the $Sr_4Mn_3O_{10}$ structure is also superimposed on the simulated image. It can be seen that the Sr projected rows appear as bright spots

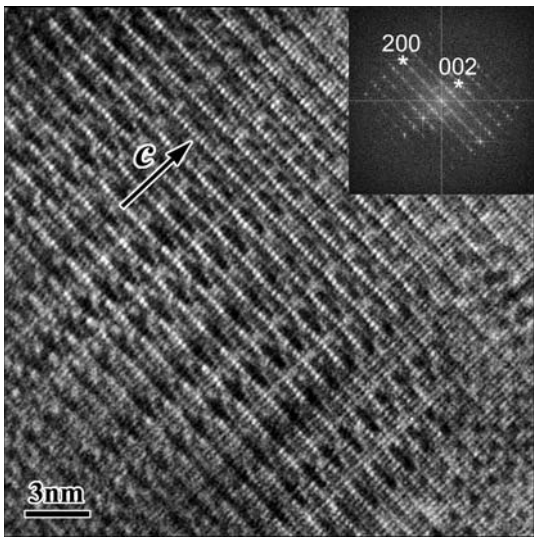

Fig. 6 A [010] HRTEM image of $La_{0.15}Sr_{3.85}Mn_3O_{10}$, showing another type of modulated structure. From the image one can see that this modulated structure is clearly associated with *periodic* lattice distortion

along the *a** direction with incommensurate feature. The *periodic* lattice distortion resulting in the structure modulation is led usually by ordered deficiency of atoms.

EELS studies were also performed on those modulated structures as well as the perfect phase. In order to make the description simple, the perfect $La_xSr_{4-x}Mn_3O_{10}$ phase is denoted as A, the La ordered modulated structure denoted as B, and the modulated structure associated with *periodic* lattice distortion (as shown in Fig. 6) denoted as C. The EELS spectra obtained from those forms are shown, respectively, by curves A–C in Fig. 7a and each spectrum includes the O-K, Mn-$L_{2,3}$ and La-$M_{4,5}$ absorption edges. All the spectra were collected along the [010] zone-axis direction in image mode. The enlarged Mn-$L_{2,3}$ edges after subtracting the backgrounds are given in Fig. 7b. From Fig. 7a we can calculate the Mn/La ratios for all spectra, and the obtained results for those spectra are very similar, indicating no enrichment or depletion of La for the modulated structures as compared to the perfect phase. From Fig. 7b one can see that the L_3/L_2 intensity ratios of Mn for the perfect phase and the modulated structure B appear similar, indicating that the two forms have approximately the same average Mn oxidation state according to the well known relationship between the L_3/L_2 intensity ratio and the valence state for Mn ions [22]. As compared with the perfect phase and the modulated structure B, the modulated structure C has a clearly higher Mn L_3/L_2 intensity ratio (see Fig. 7b), indicating that the manganese in this structure shows up a lower valence state. This decrease of Mn valence state is naturally explained as the oxygen deficiency since the perovskite framework usually allows vacancies, but not interstitials.

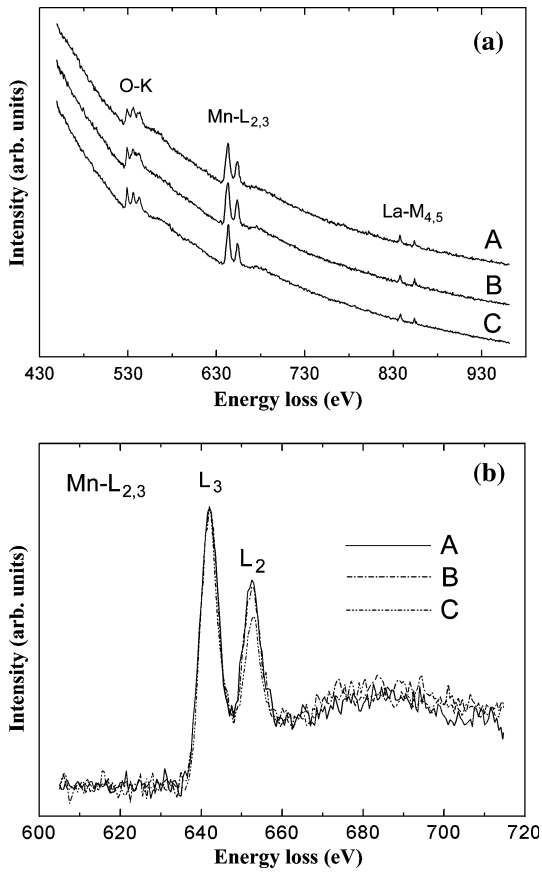

Fig. 7 (**a**) The EELS spectra obtained from the perfect phase (curve A), the La ordered modulated structure (curve B), and the modulated structure associated with *periodic* lattice distortion (as shown in Fig. 6) (curve C). (**b**) The enlarged Mn-$L_{2,3}$ edges after subtracting the backgrounds

The magnetic and specific heat measurements performed on the layered manganites $La_xSr_{4-x}Mn_3O_{10}$ have suggested that FM clusters are induced in the AFM matrix by La doping [15]. The formation of the FM clusters may have a correlation with the local ordering of the La atoms. In addition, the presence of ordered oxygen vacancies in some regions possibly results in the spin-glass like behavior in these defect regions. Our TEM results also drop a hint that caution should be used when interpreting the physical properties of perovskite-type manganites in terms of XRD-averaged structures observed.

Conclusions

By means of transmission electron microscopy and energy-loss spectroscopy, the structure and microstructure of the low La-doped layered manganite $La_xSr_{4-x}Mn_3O_{10}$ have been studied. The structure of the perfect phase has been identified as an $n = 3$ layered structure of the hexagonal series by ED, HRTEM and image simulation. The presence

of local La ordering phenomenon in the compounds was revealed by electron diffraction and high-resolution electron microscopy. This ordering of La atoms results in a two-dimensional superstructure modulation with two primary modulation vectors $q_1 = (1/4)a^*$ and $q_2 = (1/2)c^*$. In the $La_{0.15}Sr_{3.85}Mn_3O_{10}$ phase, another type of modulated structure resulting from an ordered oxygen deficiency revealed by EELS was occasionally observed.

Acknowledgments This work was supported by the National Natural Science Foundation of China (Grant Nos. 50471053, 50321101 and 50332020), the State Key Development Program for Basic Research of China (Grant Nos. 2005CB623602 and 2005CB724402), the Development Program for Scientific Research of Lanzhou University of Technology (Grant No. SB10200701), and Natural Science Foundation of Gansu Province (3ZS061-A25-039).

References

1. Kusters RM, Singleton J, Keen DA, McGreevy R, Hayes W (1989) Physica B 155:362
2. von Helmolt R, Wecker J, Holzapfel B, Schultz L, Samwer K (1993) Phys Rev Lett 71:2331
3. Jin S, Tiefel TH, McCormack M, Fastnacht RA, Ramesh R, Chen LH (1994) Science 364:413
4. Ruddlesden SN, Popper P (1958) Acta Crystallogr 11:541
5. Boulahya K, Parras M, Amador U, González-Calbet JM (2004) Solid State Ionics 172:543
6. Battle PD, Green MA, Lago J, Millburn JE, Rosseinsky MJ, Vente JF (1998) Chem Mater 10:658
7. Lago J, Battle PD, Rosseinsky MJ (2000) J Phys: Condens Matter 12:2505
8. Yu RC, Li S, Zhu JL, Li FY, Zhang Z, Jin CQ, Voigt-Martin IG (2001) J Appl Phys 90:6302
9. Floros N, Hervieu M, van Tendeloo G, Michel C, Maignan A, Raveau B (2000) Solid State Sci 2:1
10. Zubkov VG, Tyutyunnik AP, Berger IF, Voronin VI, Bazuev GV, Moore CA, Battle PD (2002) J Solid State Chem 167:453
11. Schmidt R, Pebler J, Babel D (1992) Eur J Solid State Inorg Chem 29:679
12. Boulahya K, Parras M, González-Calbet JM, Martinez JL (2002) Chem Mater 14:4006
13. Yang H, Yang RF, Li QA, Li FY, Jin CQ, Yu RC (2006) J Phys Chem Solids 67:2365
14. Boulahya K, Parras M, González-Calbet JM, Amador U, Martinez JL, Fernaández-Díaz MT (2004) Phys Rev B 69:024418
15. Tang YK, Ma X, Kou ZQ, Sun Y, Di NL, Cheng ZH, Li QA (2005) Phys Rev B 72:132403
16. Abakumov AM, Rozova MG, Antipov EV, Hadermann J, Tendeloo GV, Lobanov MV, Greenblatt M, Croft M, Tsiper EV, Llobet A, Lokshin KA, Zhao YS (2005) Chem Mater 17:1123
17. Li J, Ong CK, Liu JM, Huang Q, Wang SJ (2000) Appl Phys Lett 76:1051
18. Liu JM, Ong CK (1998) Appl Phys Lett 73:1047
19. Stadelmann PA (1987) Ultramicroscopy 21(2):131
20. Cowley JM, Moodie AF (1957) Acta Cryst 10:609
21. Scherzer O (1949) J Appl Phys 20:20
22. Wang ZL, Yin JS, Jiang YD (2000) Micron 31:571